THE INFLUENCE OF PIER GEOMETRY AND DEBRIS CHARACTERISTICS ON THE ACCUMULATION OF WOODY DEBRIS AT BRIDGE PIERS

Diego Panici[1] and Gustavo A.M. de Almeida[2]

[1]University of Southampton, University Road, Southampton, SO17 1BJ, UK. Email: d.panici@soton.ac.uk

[2]University of Southampton, University Road, Southampton, SO17 1BJ, UK

ABSTRACT

This paper analyses the influence of the geometry of bridge piers and the geometry of the supplied debris on the formation and growth of wood debris jams at bridge piers. A total of 162 laboratory experiments have been conducted. Experimental results showed that the maximum size of debris jams formed by the accumulation of cylindrical debris (i.e. wooden dowels) is smaller than that of jams formed by natural non-branched wood of irregular shape. In addition, experiments with branched debris resulted in jams that were significantly smaller and less stable than those with non-branched natural debris. Finally, comparison of experiments conducted with six different pier shapes indicate that the shape of a pier has negligible effects on the maximum size of a woody debris jam. The only exception to this observation was for square piers, which showed slightly larger debris jam sizes than the other types of piers tested.

INTRODUCTION

Bridges piers resting on mobile river beds have long been the object of concerns among hydraulic and structural engineers. The obstruction imposed by the pier reduces the flow area, alters the flow field around the pier, and produces backwater effects and localised scour. These problems

have been extensively studied over the last decades (e.g. *Melville and Sutherland*, 1988; *Dargahi*, 1990; *Williamson*, 1996; *Johnson and King*, 2003; *Dey and Raikar*, 2007), and numerous models have been developed to aid the assessment of flood risk and the design of resilient pier foundations. In many rivers, the accumulation of large woody debris (hereafter referred to as LWD) during floods can critically exacerbate the above effects. Previous studies have shown that debris jams can significantly reduce the flow area (*Parola et al.*, 2000; *Daniels and Rhoads*, 2004; *Bradley et al.*, 2005; *Pfister et al.*, 2013), which strongly affects the distribution of flow velocities and turbulence in the channel (*Gurnell et al.*, 2002; *Daniels and Rhoads*, 2004; *Wilcox and Wohl*, 2006; *Manners et al.*, 2007; *Pagliara and Carnacina*, 2011). Furthermore, debris piles produce additional hydrodynamic loadings on the pier, which combined with enhanced scour may ultimately lead to bridge failures. *Diehl* (1997) estimated that LWD accumulations contributed to about 30% of bridge failures in the US, while *Benn* (2013) found that debris was involved in 20 of the 69 bridge failures studied in the UK and Ireland. Despite these evidences, to date research on the main factors responsible for the growth of debris jams at piers are still rather limited. For many years, studies describing the dimensions of large wood accumulations were limited to field observations (*Diehl*, 1997; *Lyn et al.*, 2007; *Lagasse et al.*, 2010). Unfortunately, most of the time this type of site observations can only provide a snapshot of the problem, which may lead to an underestimation of the maximum potential size that accumulations can actually reach during an event. The shape of jams observed during these site surveys has been generically described as an inverted half-cone (*Abbe and Montgomery*, 1996; *Diehl*, 1997; *Lagasse et al.*, 2010). In addition, debris piles have been observed to grow through the successive collection of individual elements rather than bursts of logs (*Diehl*, 1997; *Bradley et al.*, 2005; *Lyn et al.*, 2007; *Lagasse et al.*, 2010). Laboratory experiments have also been conducted on debris in rivers, but to date, the large majority of these studies has focused on analysing the effects of debris jams on flow and, especially, on scour. In addition, debris trapping and growth have been experimentally studied for tsunami events (*Pasha and Tanaka*, 2016; *Stolle et al.*, 2018). Because of the lack of precise information about the size reached by accumulations, debris piles used in debris-induced scour experiments were typically modelled by idealised jam

shapes of arbitrary size. For example, *Melville and Dongol* (1992) modelled the LWD pile with a cylinder, while *Pagliara and Carnacina* (2011) used a rectangular shape. On the other hand, *Lagasse et al.* (2010) tested several shapes, e.g. a wedge with external protrusions with the aim of including the inherent irregularities of debris jams. While these studies provide interesting insights into scour induced by woody debris, the accuracy of the results obtained so far may have been strongly affected by the arbitrary shape and size adopted. A recent study by the authors (*Panici and de Almeida*, 2018) provided an experimental analysis of the actual process of formation of debris jams at single isolated piers. The study included 570 experiments in which debris jams were formed by the successive accumulation of individual elements transported by the flow. During these tests, jams gradually increased in size, although sometimes elements were removed from the jam by the flow (either individually or in groups) therefore reducing the size temporarily. However, the results from these tests showed that jams were removed from the pier by the flow (a condition hereafter referred to as *failure*) when their size was the largest observed during the course of each experiment. Using this dataset, they found relations between the maximum dimensions of debris jams (i.e. width, height, and length) and variables representing the flow and debris characteristics, which recently informed new experiments on pier scour (*Ebrahimi et al.*, 2018). The study by *Panici and de Almeida* (2018) found that the dimensionless group $Fr_L = v/\sqrt{gL}$ (where v is the average flow velocity at the pier section prior to the formation of the debris jam, and L represents the length of debris pieces) played a central role in determining the maximum dimensions of the accumulation, while other variables (e.g. pier diameter) showed little or no effect on the jam formation for the flow and debris conditions tested. Despite the large number of experiments conducted by the authors, there are still many factors that have not been thoroughly investigated and which can influence the growth of debris jams at piers. An example of this is related to the characteristics of debris elements that were used in the experiments. *Panici and de Almeida* (2018) used non-branched defoliated sticks, whilst the presence of branches was previously observed to have important effects on anchoring debris at bridge decks (*Schmocker and Hager*, 2011) and piano key-weirs (*Pfister et al.*, 2013) (resulting in increased probability of entrapment). On the other

hand, different experimental studies used wooden dowels to model debris elements. For instance, *Rusyda et al.* (2014) tested the accumulation of debris pieces produced by the instantaneous release of a large number of dowels (100 and 200) into a 30 cm wide flume, and related the accumulation volume to the frontal area obstructed by the flow. *Gschnitzer et al.* (2017) performed a series of experiments with the purpose of analysing the accumulation of woody debris for different models of bridges using dowels, dowels with protrusions, and fine material. The results were used to develop a probabilistic approach to bridge blockage by woody debris. On the other hand, *Lyn et al.* (2003) advised that natural sticks should be preferred to dowels for experimental analyses, on the basis of experiments conducted to determine the likelihood of debris accumulations being formed at piers. To date, it remains unclear the extent to which certain geometrical characteristics of individual debris elements may influence the maximum dimensions of formed debris jams.

Another important gap in current knowledge relates to the potential influence of the shape of piers on the dimensions of formed jams. The vast majority of laboratory studies conducted to date on woody debris accumulations adopted circular piers. However, *Diehl* (1997) suggested that the shape of the pier can have an important influence on the process of formation of large wood jams. In particular, the study, based on field observations, indicated that round piers are generally less prone to jam formation and proposed that their use is preferable for reducing LWD-related risks, although no factual evidence in support of this recommendation was provided. A recent study by *De Cicco et al.* (2016) was aimed at estimating the probability of entrapment of debris elements (modelled by dowels) at bridge piers varying pier shape. Six different shapes were tested, namely of circular, square, triangular, trapezoidal, ogive, and stadium section. The authors concluded that a square shape is more prone to accumulate LWD elements, whereas no noticeable differences were found for the other shapes. However, it remains largely unknown what influence the pier shape might have on the growth of debris jams after the initial debris entrapment, as well as on the final size of the accumulated debris.

The present article focuses on the experimental evaluation of the influence of the geometry of

the pier and the characteristics of debris on the growth of debris piles at bridge piers. In particular, this study is aimed at continuing and extending the work by *Panici and de Almeida* (2018) by performing laboratory tests that will elucidate the questions raised above, which are fundamental to the development of accurate models to predict the potential size of debris accumulations formed during floods.

METHODOLOGY

The experimental tests presented in this study were performed using the same experimental facilities and procedure described in *Panici and de Almeida* (2018). Tests were carried out at the University of Southampton Hydraulic laboratory in a 22 m-long and 1.375 m-wide tilting flume. The use of the same facility allowed replication of experimental conditions previously tested by the authors under similar flow velocities and depths. Table 1 shows a summary of the main characteristics of the groups of experiments performed. Experiments involving debris elements of different shapes (i.e. dowels and two different types of branched debris) were tested by experimental groups B1 to B3, whereas experiments with different pier shapes were tested by groups P1 to P6. For each group, a number of experiments were conducted in which the flow conditions were varied by adjusting the discharge and the downstream flap gate.

Debris pieces were modelled by four different types of elements. Figure 1 shows an example of each of the debris types used in this work. The figure also shows the two main geometrical variables used to describe the length of the main branch L and the branch extension b (i.e. distance normal to the direction of the main branch to the tip of the secondary branch). The debris length L and diameter d of all debris elements used in these experiments were kept constant, namely L=375 mm and d=11.85 mm (on average, standard deviation of 1.24 mm). The only exception to this was group B1, in which a diameter d=12 mm was used because of commercial availability of dowels. From the results of *Panici and de Almeida* (2018), it can be safely assumed that this small difference in diameter will have negligible influence on the comparisons reported in this paper. For natural debris (which inherently displays small variations in diameter), the reported diameter was obtained

as the average of two measures taken at both ends, which were performed using a digital calliper (accuracy ±0.1 mm).

Groups B1-B3 were aimed at analysing the influence of shape complexity on the process of entrapment of individual debris pieces and the growth of the jam. The different types of debris used in these experiments are shown in Figure 1. The lowest level of complexity is represented by dowels (B1), which are perfectly cylindrical and have a smooth surface. The next level of shape complexity is represented by non-branched natural sticks (groups P1-P5 and also other experiments in *Panici and de Almeida* (2018)) which are not perfectly straight, may display slight variations of diameter and are rougher than dowels. The introduction of branches is used to add further complexity to the geometry of the wood debris. In general, the complexity of debris shapes that can be found in nature is of difficult definition due to the many combinations of number of branches (and sub-branches) and their corresponding dimensions. For this reason, in this work a pragmatic approach is adopted where only single-branched debris pieces (i.e. natural sticks with a single branch) are tested. However, the potential influence of the size of branches has been analysed by using two values of the distance b (as shown in Figure 1). Namely, groups B2 and B3 were characterised by values of the dimensionless branch extension β=b/L of β=0.25 and β=0.50, respectively. The values of β were arbitrarily selected in order to evaluate the potential influence of this variable on the jam size in a broad range. For groups P1 to P5, debris was modelled using non-branched and defoliated natural sticks. The density of the material used for all experiments had values in the range 450-550 kg/m^3. The material employed to model woody debris also showed no visible signs of deformations over the curse of the experiments.

The model pier used for experiments B1, B2, and B3 was a circular PVC (polyvinyl chloride) cylinder of diameter D=50 mm. Experimental groups P1 to P5 were focused on the effects of pier shape on the growth and maximum size of LWD jams. In this paper, five of the shapes studied by *De Cicco et al.* (2016) were replicated with some minor differences. Figure 2 shows the detailed

cross-sections for piers used in experimental groups P1 to P5. All pier shapes were built with the same width (projected dimension in the direction normal to the main flow direction) of 50 mm, as shown in Figure 2. For group P1, a square pier of side 50 mm was used, whereas for P2 a triangular section having internal angle at the upstream vertex of 45°was used. Experimental group P3 tested an ogive-shaped pier, the function of which was based on the von Kármán ogive (that is used for minimising drag (*Pert*, 2013)). For groups P4 and P5, cross-sections used were respectively a regular trapezoid (minor and major bases of 25 mm and 50 mm), and a half-circle of diameter 50 mm. The pier used for experiments in group P1 was a square rod of PVC, while piers for groups P2 to P5 where made by 3D-printed hollow shells. These were then filled with fine and medium aggregate concrete and coated with bituminous paint in order to leave a surface finish comparable to the other PVC piers.

Pier models were placed at the flume centreline, 11 m downstream from the inlet. This distance ensured that fully developed flow conditions were reached, according to previous works conducted in the same flume. Discharge was measured by a multi-cell multi-beam ADV placed 6 m downstream of the pier. An ultrasonic probe was placed 1 m upstream of the pier in order to measure the upstream water level. Three video-cameras were used to record the time evolution of the accumulations, in order to completely describe the process of formation and growth. Two of these cameras were placed upstream from the pier, positioned respectively on the top of the flume and laterally (outside the glass walls). The third camera was placed underwater, 0.60 m downstream from the pier, and was held by a thin bar. Its size (a cylindrical camera of 35 mm diameter) and position in the wake of the pier-debris system, reduced its effects on the upstream flow. Prior to each experiment, images of a reference mesh were recorded by the three cameras, which allowed accurate measures of the jam size to be obtained from the footage. Detailed measurements of the dimensions of the accumulations were performed at the onset of the failure stage, since this was observed to be the condition when the size of jams were maximum for the vast majority of the experiments (*Panici and de Almeida*, 2018). The size of the jam was estimated by superimposing

to the reference mesh the image frames obtained from the video recordings. Each measure was taken up to half of the mesh size; hence, with an approximate accuracy of a quarter of the mesh size for each camera, i.e. 2.5 mm for the top camera and 3.2 mm for the submerged and lateral cameras. The mesh for the top camera was captured at several heights, so that the dimensions of the accumulations could be accurately determined for different depths of water. When the height was not available, a linearly interpolated measure between the two nearest heights was employed. For improved accuracy, the measured size was always cross-checked between two cameras.

In all experiments, each debris element was individually introduced into the flume 7 m upstream from the pier, at the flume centreline and from a height of (approximately) 50 mm from the water surface and kept parallel to the average flow direction. Debris feeding frequency was kept approximately constant at 20 debris/min, in order to represent an *uncongested* type of log transport (i.e. motion of individual elements that do not interact with each other) as defined by *Braudrick et al.* (1997). The introduction of debris pieces continued until the final failure of the debris jam was observed. At the downstream end of the flume, a wired mesh was placed to collect debris elements. These elements were periodically removed from the mesh to avoid backwater effects that could change the flow conditions at the pier section. In each experimental group, at least 19 different flow discharges were tested under steady flow regime. The bottom of the flume was horizontal in all tests.

The main parameter adopted for the data analysis was the debris Froude number Fr_L, which was previously observed to strongly influence the maximum size of formed jams (*Panici and de Almeida*, 2018). In particular, it has been shown that the variables $\omega^c = W^c/L$, $\eta^c = H^c/L$ and $\kappa^c = K^c/L$ (where W^c, H^c and K^c are, respectively, the width, height and length of a debris accumulation at the *critical* –i.e. at failure– stage, as sketched in Figure 3) can be modelled as functions of Fr_L. Since the length of individual debris was constant for all experiments (L= 375 mm), values of Fr_L in this paper only varied as a function of the flow velocity of each experiment. The length of the debris pieces was based on the previous work of the authors (*Panici and de Almeida*, 2018), aimed at

representing the range of the debris length to pier diameter ratio L/D that is typically observed in real-world rivers (*Diehl*, 1997; *Lagasse et al.*, 2010). In total, 162 experiments were carried out. The values of the flow discharge used in each individual test spanned from 0.08 m^3/s to 0.42 m^3/s, which resulted in average flow velocities v in the range of 0.20 m/s to 0.81 m/s. Flow depths varied between 0.261 m and 0.412 m. For all experiments, the Froude number ($Fr{=}v/\sqrt{gh}$, where h is the water depth at the pier section prior to the debris accumulation) varied between 0.125 and 0.432 and the Reynolds number ($Re{=}\rho v h/\mu$, where ρ is the water density and μ is the dynamic viscosity) from 5.56 x 10^4 to 3.34 x 10^5.

RESULTS

The evolution of wood debris accumulations observed in the experiments followed the general patterns previously observed by *Panici and de Almeida* (2018). In particular, in all experiments debris jams were dislodged from the pier by the flow (i.e. failed) through a rotation of the jam about the pier. Moreover, in virtually all of these experiments, the maximum size of formed debris jams was observed immediately before failure. Despite these similarities, notable differences were observed between experimental groups conducted in the present study and in *Panici and de Almeida* (2018), which are described in the following sections.

Debris shape

Figure 4 compares the critical dimensions of debris jams formed by natural sticks (4a, as observed by *Panici and de Almeida* (2018)), dowels (4b, group B1), and the two branched debris (4c and 4d, groups B2 and B3, respectively) for a range of Fr_L. The figure illustrates important differences among the four types of debris studied. Qualitatively, jams formed by dowels are more densely packed and display a more regular geometry. During these experiments, for (approximately) $Fr_L{\geq}0.40$, jams could not form under any circumstances. All debris pieces were rapidly removed by the flow, and single elements were entrapped only for a very short period of time. Furthermore, even when a large number of elements (i.e. more than 15) was manually placed at the pier in the attempt to initiate an accumulation, they were rapidly dislodged from the pier. Therefore, $Fr_L{=}0.40$ can be regarded as the maximum value of Fr_L under which jams formed by this idealised type of

debris can possibly develop.

Debris accumulations formed by branched sticks displayed a different pattern. An example can be observed in figures 4c and 4d, which show two jams from groups B2 and B3 under very similar values of Fr_L. Jams formed by branched debris tended to be very unstable with frequent dislodgement of elements and size variation, and never displaying the long stable periods that were frequently observed for non-branched debris. Furthermore, the porosity (defined as the ratio of the solid volume and the overall volume) of jams formed by branched debris was significantly smaller than the porosity of jams formed with non-branched sticks although a quantitative measure was difficult to be obtained. Qualitative observations indicate that this trend depends on the dimensionless ratio b/L (i.e. visual inspections indicate that B3 experiments displayed higher porosities than B2).

Figure 5 shows the maximum width, depth, and length (made dimensionless by L) reached by accumulations formed during experiments of groups B1, B2, and B3 as a function of Fr_L. For the sake of comparison, the experimental results of *Panici and de Almeida* (2018) for uniform length debris jams formed by natural sticks are also displayed on the same figure. At the lowest range of Fr_L (e.g. for $Fr_L \leq 0.20$), jams formed by dowels (group B1) reach maximum dimensions comparable to those previously observed for natural non-branched debris, i.e. $\omega^c \approx 2.7\text{-}3.0$, $\eta^c \approx 0.2$, and $\kappa^c \approx 1.5$. However, at larger Fr_L the jam dimensionless width ω^c, and length κ^c display a notable drop compared to the corresponding values obtained with natural sticks. At the highest range of Fr_L, the values of ω^c, η^c, and κ^c are approximately 1.1, 0.25, and 0.2, respectively.

The maximum size reached by branched jams (groups B2 and B3) also displays important differences compared to non-branched sticks. In Figure 5, the comparison of the results from experiments with and without branches shows that for $Fr_L < 0.20$ jams formed by branched sticks are considerably narrower (up to 35% less) than jams made of non-branched elements. For example, at low Fr_L jams of group B3 showed a maximum dimensionless width ω^c of approximately 1.9,

whereas values for non-branched sticks ranged between 2.5 and 3.2. Although this difference is more clearly observed for ω^c, the same tendency (albeit less marked) also holds true for η^c and κ^c, with the latter being the least affected. With increasing values of Fr_L, differences in ω^c for non-branched and branched debris are reduced to approximately 20%. Differences between jams formed by debris elements with branches of different length (i.e. groups B2 and B3) are less pronounced than with non-branched elements, although the values of ω^c in B3 are in general smaller than those of B2.

Pier shape

Unlike debris shape, varying the shape of the pier had minor or negligible effects on the formation and maximum size of large wood piles. Qualitatively, jams accumulated on piers of groups P1 to P5 showed consistency with those formed at the circular pier adopted by *Panici and de Almeida* (2018). Namely, growth of debris accumulations started with the *unstable* phase (i.e. a quick and unordered growth of the jam), followed by a longer *stable* phase (i.e. a jam growth showing little changes and high stability), and concluded by the final rotational motion of the *critical* phase (i.e. the rotation and dislodgement of the debris jam from the pier). No substantial differences were observed with regards to this formation process, with the exception for piers with flat surfaces (i.e. square in group P1 and trapezoidal in P4). These groups were typically more efficient in recruiting debris at the early stages of the jam formation, which reduced the duration of the *unstable* phase. However, the results provided in this paper show that the shape of the pier has only a minor influence on the final, maximum dimensions of formed jams, as described below.

Figure 6 shows the maximum size of accumulations as a function of Fr_L for groups P1 to P5, along with the data from *Panici and de Almeida* (2018) for circular piers. Overall, these results for ω^c and $\kappa^c$of all tests lie on the same scatter band previously obtained for a circular pier, except for square piers, which resulted in wider and longer debris accumulations. The depth of accumulations formed at all pier shapes lie on the same band, and no significant differences can be attributed to any particular shape. At the lowest values of Fr_L tested (i.e. say, $0.12 \leq Fr_L \leq 0.15$), ω^c for experiments

in groups P2-P5 ranged between 2.4~3.1, η^c between 0.04~0.08, and κ^c between 1.2~1.6, all of which falling within the range of scatter of results obtained with circular piers. For increasing Fr_L, ω^c and κ^c decrease non-linearly, whereas η^c increases. Around the highest value of Fr_L studied in this work (i.e. $Fr_L \approx 0.42$) ω^c for P2-P5 ranges between 1.4~1.9, η^c between 0.35~0.55, and κ^c between 0.50 ~0.90.

DISCUSSION

The experimental results shown in the previous section provide new insights on the phenomenon of woody debris accumulations at bridge piers. At first, the general observations of the jams growth phases from this study are consistent with previous experimental results. The new results shown in this paper have also confirmed that the failure phenomenon is ubiquitous, and occurs for all shapes of debris and piers tested. Nonetheless, some important differences were observed when the results of the experiments conducted in this study (with debris and piers of different shapes) were compared against those previously conducted with natural sticks and circular piers (*Panici and de Almeida*, 2018), which motivates the discussion below.

The use of dowels to model natural woody debris in rivers needs to be carefully re-considered for a number of reasons. First, dowel jams never formed for $Fr_L \geq 0.40$, which is lower than the maximum values of $Fr_L \approx 0.5$ for which an accumulation of natural sticks was experimentally observed to develop. In addition, accumulations formed by dowels are smaller than those formed by natural sticks, particularly when $Fr_L \geq 0.25$. Another difference was observed for the shape and disposition that debris assume. The regular structure displayed by the accumulation of dowels may not be representative of real-world jams that are formed by natural wood drifts, which –as field observations show– display a less regular shape. For these reasons, results reported in this paper provide evidence in support of previous recommendations by *Lyn et al.* (2003), who suggested that use of dowels should be avoided for experimental studies on LWD accumulations.

Debris jams formed by branched sticks were considerably smaller and less stable than those

formed by non-branched elements. This is counter-intuitive, as branches are expected to provide interlocking and therefore robustness to the accumulation. Here the authors propose a hypothesis that would potentially explain this observed behaviour. The asymmetry between the two semi-widths on the left and right (W_L and W_R are used to denote the left and right distances, normal to the streamwise direction, from the pier's axis to the tips of the accumulation, as depicted on Figure 3) has previously been raised by *Panici and de Almeida* (2018) as a primary factor inducing the torque required to dislodge the debris jam from the pier. During the experiments presented in this paper, it was qualitatively observed that during tests in groups B2 and B3, the planar asymmetry varied widely as new debris pieces were collected. Namely, the widest side of the accumulation changed from one side to the other several times during the experiments. The reason for this behaviour is related to the higher porosity of jams formed by branched debris. High porosity values mean that each element's contribution to increasing one semi-width is higher, leading to a more discontinuous growth and increased probability of large asymmetries being formed by chance, which causes the inherent instability of the branched debris jam.

The results of the experiments with different pier shapes presented in this work show that the pier shape does not substantially influence the dimensions of formed debris jams. The only exception to this rule was observed for squared piers, which displayed widths and lengths approximately 15% larger than the other groups. This last observation, combined with previous findings by *De Cicco et al.* (2016), who concluded that square piers are more likely to entrap debris elements, indicates that piers of square shape should be avoided in rivers where debris accumulations may occur.

The data shown in figures 5 and 6 has been also analysed for a regression (shown in the figures). Using a maximum likelihood estimation (MLE) approach, the resulting regressions coefficients are represented in Tables 2, 3, and 4, in which the type of regression function was selected employing the same by *Panici and de Almeida* (2018) of the type $a+be^{-cFr_L}$, where a, b, and c are regression coefficients.

In all of the experiments reported in this paper the width of the flume B was fixed (1.375 m), but the jam-to-flume ratio W/B changed according to the variation of W. At failure conditions, values of W/B ranged 0.29 from 0.83, and in more than 90% of the tests W/B was well below 0.70. It was also observed that even during those few experiments in which W/B reached values higher than 0.70, the failure mechanism was essentially identical to the failure observed at lower W/B ratios (i.e. a rotational motion without direct contact between debris and the flume walls). The resulting dimensions of debris formed with $W/B>0.7$ were also within the same band as the results obtained at $W/B<0.7$. We therefore assume that any potential interactions between the flow and the walls of the flume were negligible in all experiments. In addition, the maximum backwater increase induced by the formed debris jams was approximately 1.29% for groups B1 to B3 and a maximum of 7.15% for groups P1 to P5 (although this higher value was only observed during two tests, whilst in all the other tests the water level increased by less than 4.1%). We therefore assume that the results of our experiments represent the condition of an isolated pier. Further experiments are required to study the more complex situation where the blockage ratio is high enough to induce considerable changes in the upstream free surface elevation and in the process of formation and failure of debris jams.

CONCLUSIONS

A detailed analysis of the different factors affecting the formation of woody debris jams at bridge piers is key to the development of a robust theory and models to estimate the maximum dimensions that can be potentially formed at bridge piers. This article experimentally analysed the influence of the geometry of debris elements and bridge piers on the process of formation and growth of debris jams at piers, with particular focus on the maximum size of formed accumulations. A total of 162 new experiments were conducted, the results of which were compared against the results of other 570 experiments recently published.

It has been observed that debris jams formed by dowels (i.e. perfectly cylindrical debris) tend to reach sizes that are comparable to those formed by natural sticks only for the lowest range of

the debris Froude number $Fr_L = v/\sqrt{gL}$. However, at the highest range of Fr_L, jams formed by debris modelled by dowels can be up to 40% smaller than those formed by natural sticks. Moreover, dowels jams could not be formed for Fr_L>0.40. Under these conditions, elements were promptly removed from the pier by the flow, even if attempts were made to place them manually at the pier as a large bunch. These observations pose an important question about the accuracy of experimental studies that are based on jams formed by debris modelled with dowels. On the other hand, the results of experiments with branched debris elements showed that branches play a significant role on the formation process. Accumulations of this kind were observed to be less stable than those formed by non-branched sticks, displaying frequent early failures and a continuous change of the jam shape. Furthermore, the maximum size reached by branched jams was significantly smaller than those formed by non-branched natural sticks, with differences up to 35% for ω^c, at the lowest range of Fr_L. Thus, non-branched sticks can be considered as an idealised situation in which the formed accumulations constitute a worst-case scenario for practical applications.

The results of the comparative analysis presented in this paper, which included six different pier shapes, revealed that the dimensions of the formed debris jams are not significantly influenced by the shape of the pier. The maximum size reached by the jams tested in this study was within the same values that were previously reported for circular piers. A relatively minor exception to this conclusion was observed for the square shape. In this case, the maximum width of the accumulation was approximately 15% larger than the corresponding width found for accumulations with other shapes. Square piers were also observed to initiate the accumulation process more rapidly.

ACKNOWLEDGEMENTS

The authors received financial support for this research by the UK Engineering of and Physical Sciences Research Council (EPSRC) through the Centre for Doctoral Training in Sustainable Infrastructure Systems (CDT-SIS), grant EP/L01582X/1. Part of this research was also funded by the UK Natural Environment Research Council (NERC), grant NE/R009015/1. The authors are grateful to

401 Dr Toru Tsuzaki and Mr Karl Scammell of the University of Southampton Hydraulics Laboratory
402 for the technical and material support in carrying out the experiments, and are also thankful to the
403 MSc student Matthew Choi for helping with part of the experimental work. Data supporting the
404 results presented in this paper are openly available from the University of Southampton repository
405 at doi: http://doi.org/10.5258/SOTON/D0916.

406 **REFERENCES**

407 Abbe, T.B., and D. Montgomery (1996), Large woody debris jams, channel hydraulics and habitat
408 formation in large rivers, *Regulated Rivers*, *12*, 201–221.

409 Benn, J (2013), Railway bridge failure during flooding in the UK and Ireland, *Proceedings of the*
410 *Institution of Civil Engineers*, *166*(4), 163–170.

411 Bradley, J.B., D.L. Richards, and C.D. Bahner (2005), Debris control structures - evaluation
412 and countermeasures, Federal Highway Administration, U.S. Department of Transportation,
413 Washington D.C., USA.

414 Braudrick, C.A., G.E. Grant, Y. Ishikawa, and H. Ikeda (1997), Dynamics of wood transport in
415 streams: A flume experiment, *Earth Surface Processes and Landforms*, *22*, 669–683.

416 Daniels, M.D., and B.L. Rhoads (2004), Effect of LWD Configuration on Spatial Patterns of Three-
417 Dimensional Flow in Two Low-Energy Meander Bends at Varying Stages, *Water Resources*
418 *Research*, *40*.

419 Dargahi, B. (1990), Controlling mechanism of local scouring, *Journal of Hydraulic Engineering*,
420 *116*, 1197–1214.

421 De Cicco, N., E. Paris, and L. Solari (2016), Wood accumulation at bridges: Laboratory experiments
422 on the effect of pier shape, *River Flow 2016*, St. Louis, USA.

423 Dey, S., and R. Raikar (2007), Characteristics of horseshoe vortex in developing scour holes at
424 piers, *Journal of Hydraulic Engineering*, *133*, 399–413.

425 Diehl, T.H. (1997), Potential drift accumulation at bridges, Federal Highway Administration, U.S.
426 Department of Transportation, Washington D.C., USA.

427 Ebrahimi, M., P. Kripakaran, D. Prodanovic, R. Kahraman, M. Riella, G. Tabor, S. Arthur, and
428 S. Djordević (2018), Experimental study on scour at a sharp-nose bridge pier with debris
429 blockage, *Journal of Hydraulic Engineering*, *144*.

430 Gschnitzer, T., and B. Gems, and B. Mazzorana, and M. Aufleger (2017), Towards a robust
431 assessment of bridge clogging processes in flood risk management, *Geomorphology*, *279*, 128–
432 140.

433 Gurnell, A.M., and H. Piégay, and F. Swanson, and S. Gregory (2002), Large wood and fluvial
434 processes, *Freshwater Biology*, *47*, 601–619.

435 Johnson, K.R., and F.C.K. King (2003), Measurements of water surface profile and velocity field
436 at a circular pier, *Journal of Engineering Mechanics*, *129*, 502–513.

437 Lagasse, P., P. Colopper, L. Zevenbergen, W. Spitz, and L. Girard (2010), Effects of debris on
438 bridge pier scour, National Cooperative Highway Research Program, Transportation Research
439 Board, Washington D.C., USA.

440 Lyn, D., T. Cooper, Y. Yi, R. Sinha, and A. Rao (2003), Debris accumulation at bridge crossing:
441 Laboratory and field studies, Federal Highway Administration, U.S. Department of Transporta-
442 tion, Washington D.C., USA.

443 Lyn, D., T. Cooper, C. Condon, and G. Gan (2007), Factors in debris accumulation at bridge piers,
444 Federal Highway Administration, U.S. Department of Transportation, Washington D.C., USA

445 Manners, R.B., M.W. Doyle, and M.J. Small (2007), Structure and hydraulics of natural woody
446 debris jams, *Water Resources Research*, *43*, W06432, doi:10.1029/2006WR004910.

447 Melville, B.W., and A. Sutherland (1988), Design method for local scour at bridge piers, *Journal*
448 *of Hydraulic Engineering*, *114*, 1210–1226.

449 Melville, B.W., and D. Dongol (1992), Bridge pier scour with debris accumulation, *Journal of*
450 *Hydraulic Engineering*, *118*, 1306–1310.

451 Pagliara, S., and I. Carnacina (2011), Influence of wood debris accumulation on bridge pier scour,
452 *Journal of Hydraulic Engineering*, *137*, 254–261.

453 Panici, D., and G.A.M. de Almeida (2018), Formation, growth, and failure of debris jams at bridge
454 piers, *Water Resources Research*, *54*, https://doi.org/10.1029/2017WR022177.

455 Parola, A.C., C.J. Apelt, and M.A. Jempson (2000), Debris Forces on Highway Bridges, National
456 Cooperative Highway Research Program, Transportation Research Board, Washington D.C.,
457 USA.

458 Pasha, G.A., and N. Tanaka (2016), Effectiveness of finite length inland forest in trapping tsunami-
459 borne wood debris, *Journal of Earthquakes and Tsunamis*, 1650008.

460 Pert, G.J. (2013), *Introductory Fluid Mechanics for Physicists and Mathematicians*, Wiley, Chich-
461 ester, UK.

462 Pfister, M., D. Capobianco, B. Tullis, and A.J. Schleiss (2013), Debris-Blocking Sensitivity of
463 Piano Key Weirs under Reservoir-Type Approach Flow, *Journal of Hydraulic Engineering*, *139*,
464 1134–1141.

465 Rusyda, M., H. Hashimoto, and S. Ikematsu (2014), Log jam formation by an obstruction in a river,
466 *River Flow 2014*, Lausanne, Switzerland.

467 Schmocker, L., and W.H. Hager (2011), Probability of Drift Blockage at Bridge Decks, *Journal of*
468 *Hydraulic Engineering*, *137*, 470–479.

469 Stolle, J., T. Takabatake, I. Nistor, T. Mikami, S. Nishizaki, G. Hamano, H. Hishii, T. Shibayama,
470 N. Goseberg, and E. Petriu (2018), Experimental investigation of debris damming loads under
471 transient supercritical flow conditions, *Coastal Engineering*, *139*, 16–31.

Wilcox, A.C., and E.E. Wohl (2006), Flow resistance dynamics in step-pool stream channels: 1. Large woody debris and controls on total resistance, *Water Resources Research*, *42*.

Williamson, C. (1996), Vortex dynamics in the cylinder wake, *Annual Review in Fluid Mechanics*, *28*, 477–539.

List of Tables

Group	Debris used	Pier used	Number of experiments	Fr_L range
B1	Dowels	Circular	19	0.127 - 0.391
B2	Branched sticks β=0.25	Circular	19	0.124 - 0.427
B3	Branched sticks β=0.50	Circular	19	0.124 - 0.427
P1	Sticks	Square	21	0.108 - 0.419
P2	Sticks	Triangular	21	0.113 - 0.426
P3	Sticks	Ogive	21	0.116 - 0.431
P4	Sticks	Trapezoidal	21	0.121 - 0.426
P5	Sticks	Half-circular	21	0.117 - 0.423

TABLE 1. Experimental groups and variables used for the tests presented in this study.

Group	a	b	c
B1	0.568	5.191	6.003
B2 & B3	0.321	2.042	1.905
P1 to P5	-1.680	4.947	0.983

TABLE 2. Regression coefficients for ω^c.

Group	a	b	c
B1	0.345	-0.416	7.108
B2 & B3	0.367	-0.513	4.968
P1 to P5	0.578	-0.930	5.043

TABLE 3. Regression coefficients for η^c.

Group	a	b	c
B1	0.258	9.209	14.732
B2 & B3	0.454	47.015	24.232
P1 to P5	0.296	1.863	4.042

TABLE 4. Regression coefficients for κ^c.

List of Figures

Fig. 1. Types of debris elements used in this experimental study. From left to right: wooden dowel (group B1), non-branched natural stick (groups P1 to P5), branched sticks - small branch (group B2), and branched sticks - large branch (group B3).

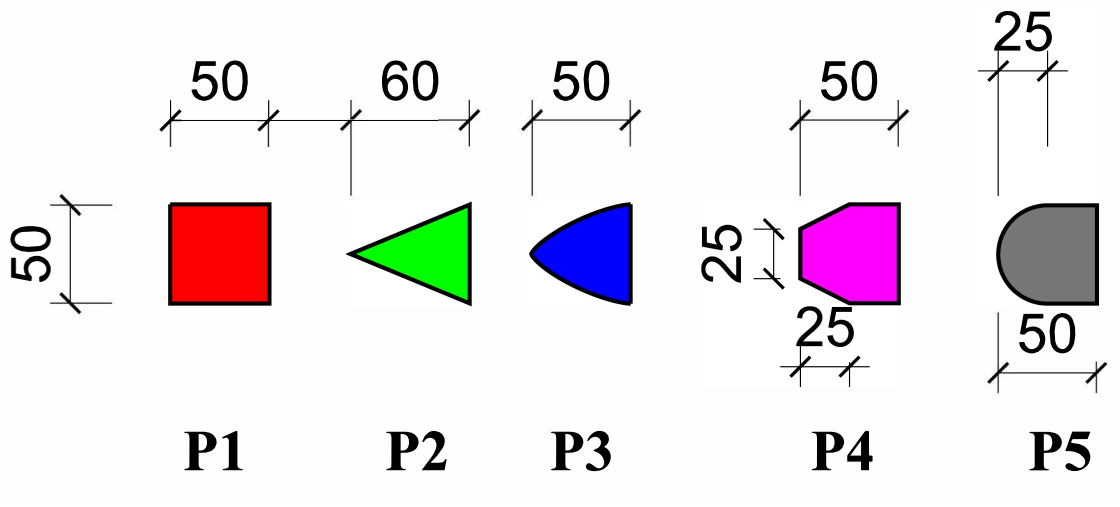

Fig. 2. Cross-sections of the piers used for experimental groups P1 to P5. Dimensions in mm.

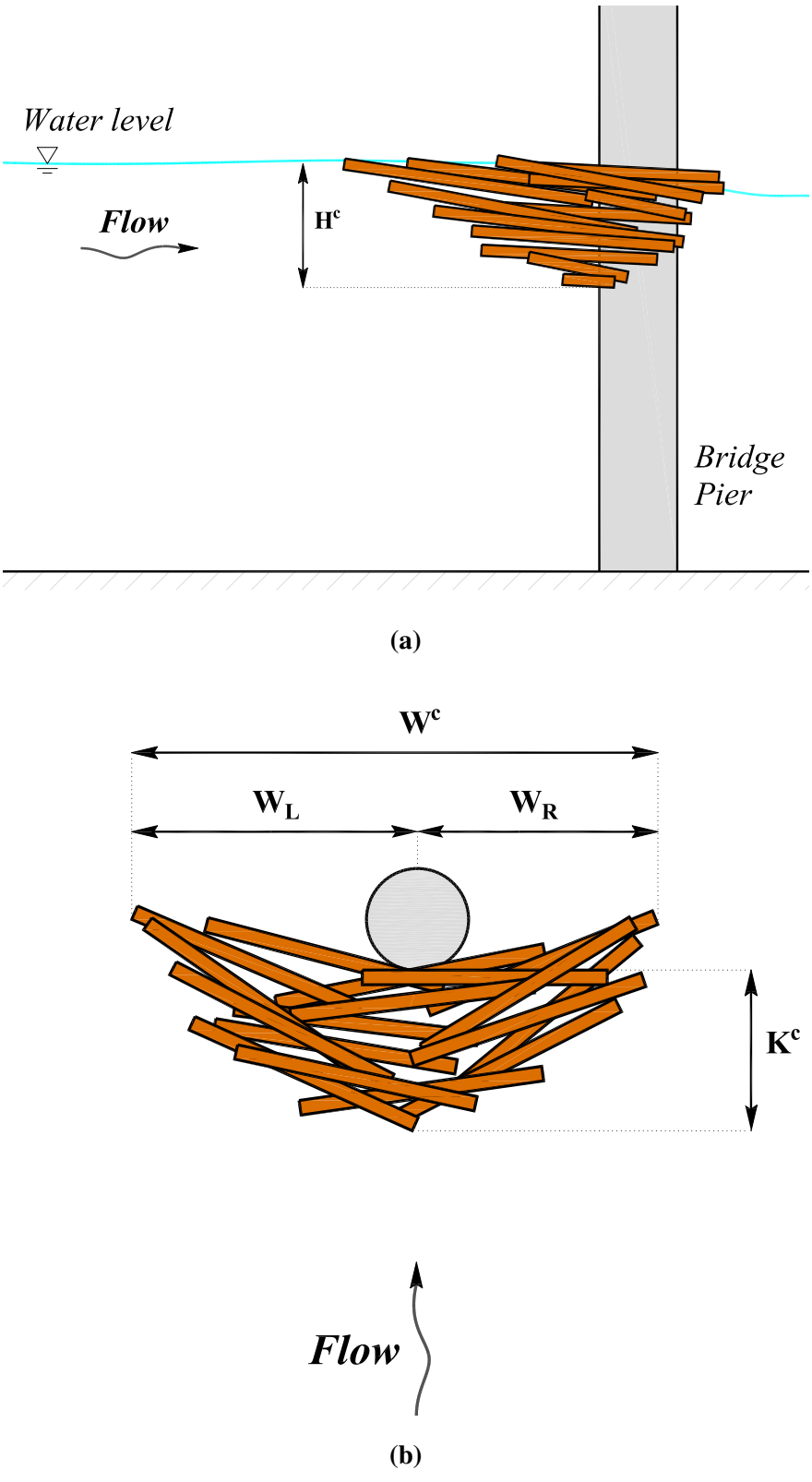

Fig. 3. Sketch (a) profile and (b) plan view of a debris jam at the onset of failure conditions.

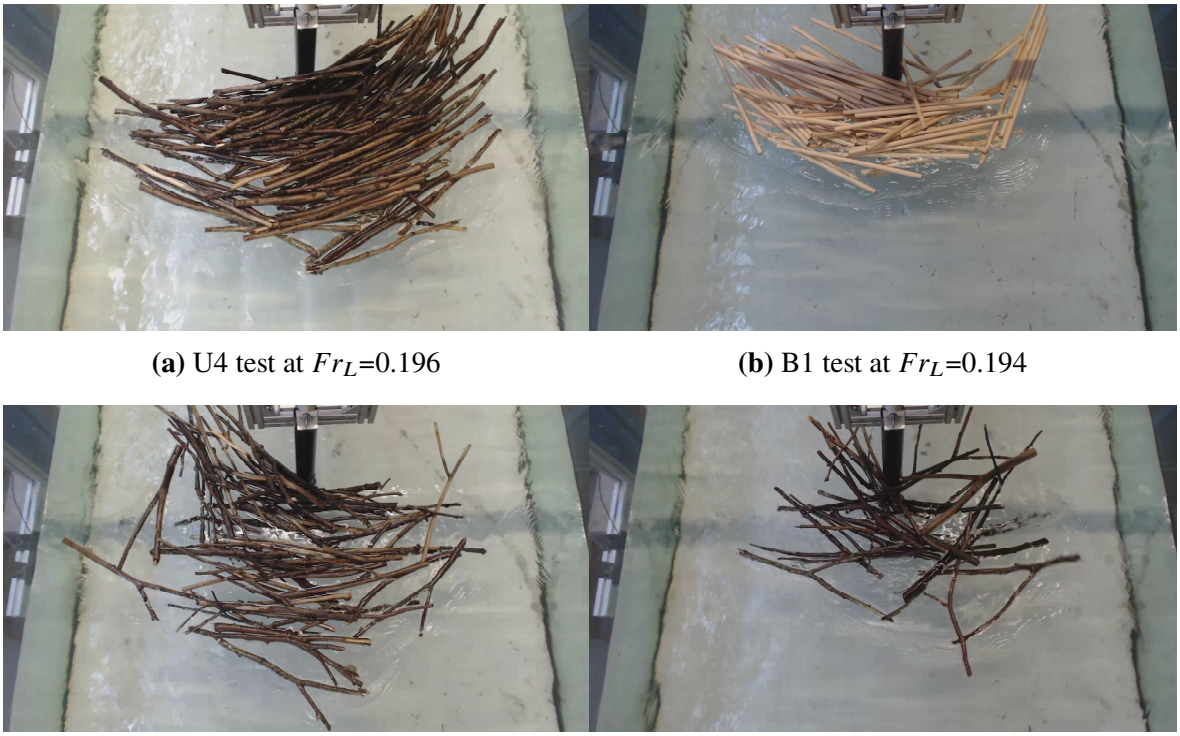

(a) U4 test at Fr_L=0.196 **(b)** B1 test at Fr_L=0.194

(c) B2 test at Fr_L=0.191 **(d)** B3 test at Fr_L=0.196

Fig. 4. Examples of accumulations before the jam failure, during experiments with non-branched debris (4a) from experiments by *Panici and de Almeida* (2018), debris jams formed by dowels in group B1 (4b), branched in group B2 (4c), and branched in group B3 (4d) for similar Fr_L and equal length and diameter of debris pieces.

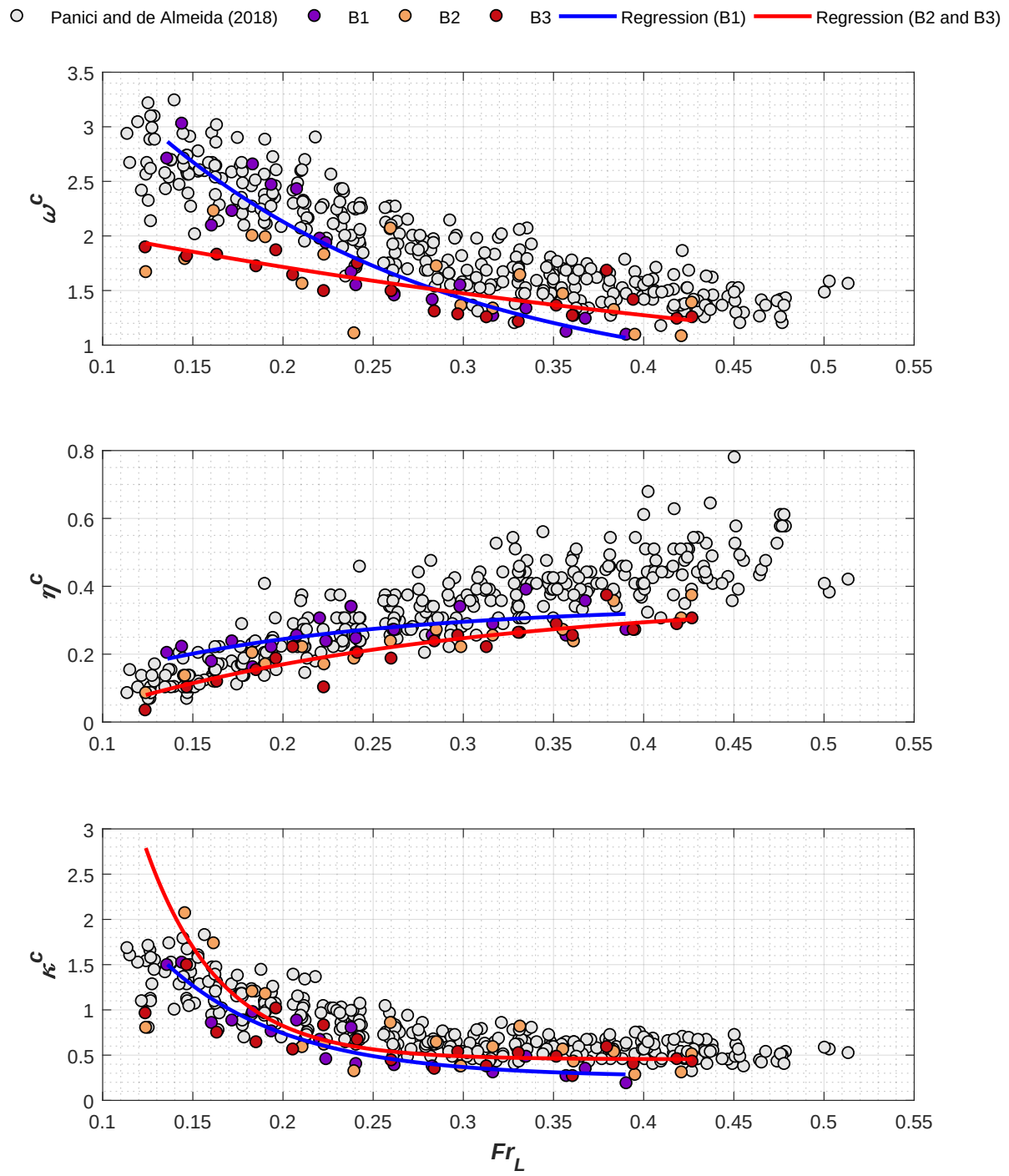

Fig. 5. Values of the dimensionless (top to bottom) width ω^c, height η^c and length κ^c against Fr_L (horizontal axis) for experimental groups B1 to B3. Data from *Panici and de Almeida* (2018) is also shown for comparison.

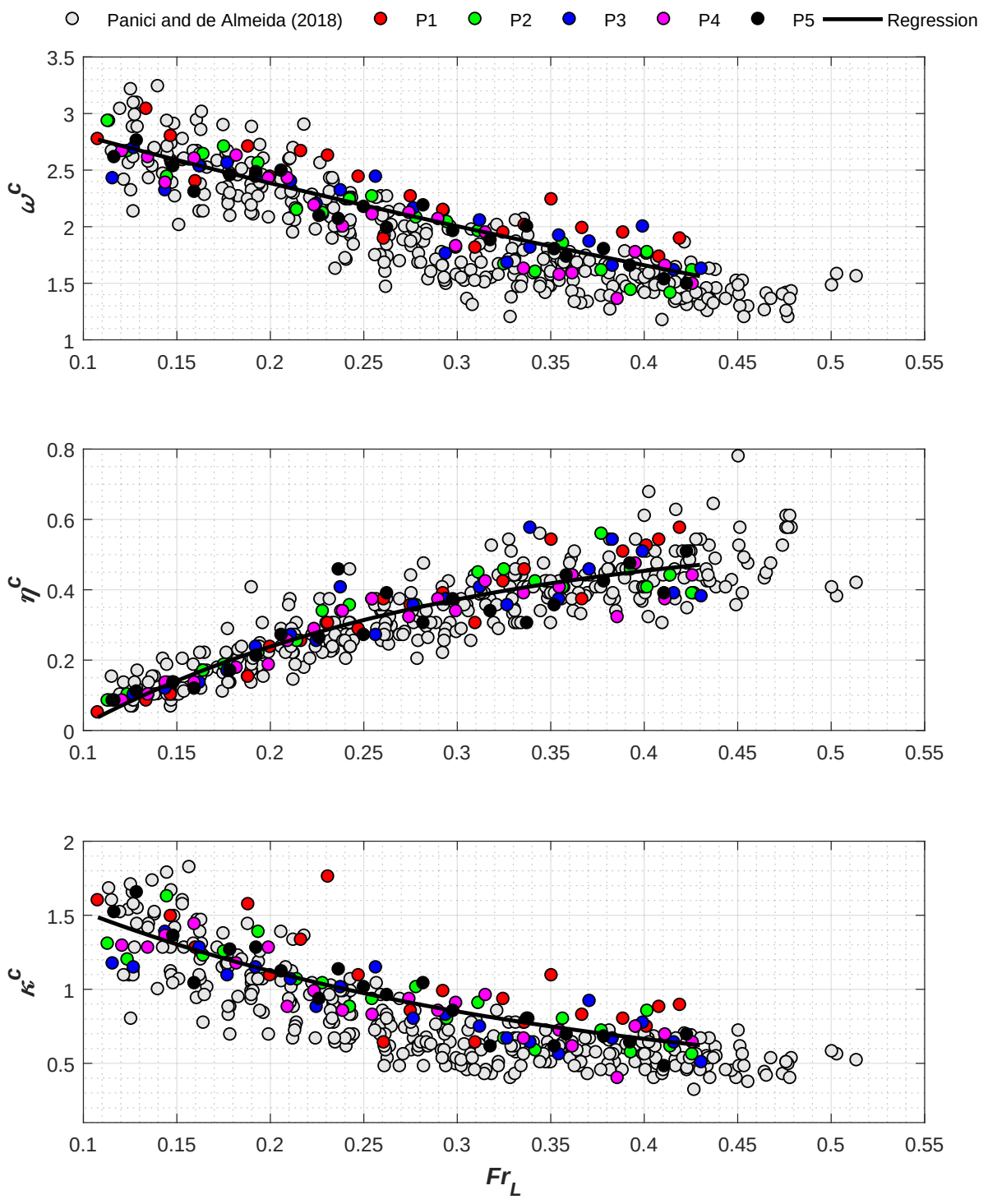

Fig. 6. Values of the dimensionless (top to bottom) width ω^c, height η^c and length κ^c against Fr_L (horizontal axis) for experimental groups P1 to P5. Data from *Panici and de Almeida* (2018) is also shown for comparison.